

Diacetylene Functionalized Covalent Organic Framework (COF) for Photocatalytic Hydrogen Generation

Pradip Pachfule, Amitava Acharjya, Jerome Roeser, Thomas Langenhahn, Michael Schwarze, Reinhard Schomaecker, Arne Thomas, and Johannes Schmidt

J. Am. Chem. Soc., **Just Accepted Manuscript** • Publication Date (Web): 29 Dec 2017

Downloaded from <http://pubs.acs.org> on December 29, 2017

Just Accepted

“Just Accepted” manuscripts have been peer-reviewed and accepted for publication. They are posted online prior to technical editing, formatting for publication and author proofing. The American Chemical Society provides “Just Accepted” as a free service to the research community to expedite the dissemination of scientific material as soon as possible after acceptance. “Just Accepted” manuscripts appear in full in PDF format accompanied by an HTML abstract. “Just Accepted” manuscripts have been fully peer reviewed, but should not be considered the official version of record. They are accessible to all readers and citable by the Digital Object Identifier (DOI®). “Just Accepted” is an optional service offered to authors. Therefore, the “Just Accepted” Web site may not include all articles that will be published in the journal. After a manuscript is technically edited and formatted, it will be removed from the “Just Accepted” Web site and published as an ASAP article. Note that technical editing may introduce minor changes to the manuscript text and/or graphics which could affect content, and all legal disclaimers and ethical guidelines that apply to the journal pertain. ACS cannot be held responsible for errors or consequences arising from the use of information contained in these “Just Accepted” manuscripts.

Diacetylene Functionalized Covalent Organic Framework (COF) for Photocatalytic Hydrogen Generation

Pradip Pachfule,^{†,§} Amitava Acharjya,^{†,§} Jérôme Roeser,[†] Thomas Langenhahn,[†] Michael Schwarze,[‡] Reinhard Schomäcker,[‡] Arne Thomas^{†*} and Johannes Schmidt[†]

[†] Department of Chemistry/Functional Materials, Technische Universität Berlin, Hardenbergstraße 40, 10623 Berlin, Germany.

[‡] Technische Universität Berlin, Institut für Chemie, TC 08, Straße des 17. Juni 124, 10623 Berlin, Germany.

Supporting Information

ABSTRACT: Covalent organic frameworks (COFs) are crystalline, highly porous, two- or three-dimensional polymers with tunable topology and functionalities. Because of their higher chemical stabilities in comparison to their boron-linked counterparts, imine or β -ketoenamine linked COFs have been utilized for a broad range of applications, including gas storage, heterogeneous catalysis, energy storage devices or proton-conductive membranes. Herein, we report the synthesis of highly porous and chemically stable acetylene ($-C\equiv C-$) and diacetylene ($-C\equiv C-C\equiv C-$) functionalized β -ketoenamine COFs, which have been applied as photocatalyst for hydrogen generation from water. It is shown that the diacetylene moieties have a profound effect as the diacetylene based COF largely outperforms the acetylene based COF in terms of photocatalytic activity. As a combined effect of high porosity, easily accessible diacetylene ($-C\equiv C-C\equiv C-$) functionalities and considerable chemical stability, an efficient and recyclable heterogeneous photocatalytic hydrogen generation is achieved.

INTRODUCTION

Porous materials such as activated carbons, zeolites, metal-organic frameworks (MOFs) or covalent organic frameworks (COFs) have been tested and utilized for a variety of applications.¹⁻⁶ Ordered crystalline materials have attracted much attention, because of the possibility to precisely predict and position atoms or functional groups within the large and accessible pore surfaces.⁷⁻⁹ Due to their unique ordered channel structures, relatively large pore apertures, high chemical and thermal stabilities, and defined chemical nature of their pore walls, COFs have received increasing interest for gas storage and separation, heterogeneous catalysis, proton conductivity, optoelectronics and energy applications.¹⁰⁻¹⁵ Using various organic building units and covalent bond forming reactions, COFs with variable porosities, functionalities and morphologies have been synthesized.¹⁶⁻²⁵ As constructed entirely from covalent bonds, COFs often show good chemical stabilities,^{14,26,27} which can be further enhanced by introducing structures which enable keto to enol tautomerism²⁸ and/or hydrogen bonding, especially in imine-linked and other nitrogen-containing COFs.^{19,29}

The synthesis of COFs with various building units such as phenyl, biphenyl, naphthalene, anthracene, pyrene, triazine, etc. have been explored in the last few years.^{15,19} Such studies have shown that, generally, the rate of COF formation decreases when larger pore sizes are obtained, probably due to the corresponding higher fraction of empty space per unit

cell, which is decreasing the interlayer attraction.³⁰⁻³² Recently, Dichtel *et al.* showed that the rate of COF growth increases with enhanced van der Waals surface and planarity of the linkers, as the stacking of the two-dimensional (2D) polymers influences the rate of COF formation.³⁰ Because of the appreciably lower activation energy, the van der Waals interactions of larger aromatic systems stabilizes the polymer stacking intermediate, which further enhances the 2D COF formation as compared to small aromatic cores. In this regard, the synthesis of highly porous 2D COFs originating from small organic cores (e.g. phenyl) separated by -ethyne (acetylene, $-C\equiv C-$), and especially by -buta-1,3-diyne (diacetylene, $-C\equiv C-C\equiv C-$) moieties, seems to be an immense challenge, as these extended organic linkers should on the one hand yield large pore sizes but on the other have very weak van der Waals interactions, and both factors does not assist for interlayer stacking of the 2D polymers, which is the rate-determining step in COF synthesis.^{30,33}

Despite that the synthesis of diacetylene-bridged COFs seem quite challenging, such structures could be of high interest especially due to their highly conjugated structures, high charge carrier mobility and ability to provide active sites for facile migration of photogenerated excitons to the surface.³⁴ Indeed materials having diacetylene moieties have received much attention in photocatalysis, optoelectronics and photo/thermochromism,³⁴⁻³⁶ and therefore polymers and small molecules having diacetylene moieties in their backbone have been explored largely.³⁶⁻³⁸ However, COFs comprised of these moieties have not been explored so far, except few examples of diacetylene-based boroxines or boronate ester-based COFs. These COFs have however not been explored for any applications, most probably due to the synthetic difficulties described above.³³

Herein, we present the synthesis of two novel β -ketoenamine COFs, TP-EDDA and TP-BDDA, bearing acetylene and diacetylene moieties, *via* an acid-catalyzed solvothermal reaction. TP-EDDA and TP-BDDA have been synthesized by the reaction of 1,3,5-triformylphloroglucinol (TP, 63 mg, 0.3 mmol) with 4,4'-(ethyne-1,2-diyl)dianiline (EDDA, 94 mg, 0.45 mmol) or 4,4'-(buta-1,3-diyne-1,4-diyl)dianiline (BDDA, 105 mg, 0.45 mmol), respectively, in the presence of 3 M acetic acid (0.5 mL) using 1:1 mesitylene/dioxane (3 mL) as the solvents [Sections S2, in the Supporting Information (SI)]. Keto-enol tautomerization provided by ketoenamine formation of amines with TP has been utilized to achieve COFs with essential chemicals stability.³⁹ In order to synthesize the diacetylene-based crystalline TP-

BDDA COF, we have carried out a series of experiments to

optimize the reaction time and

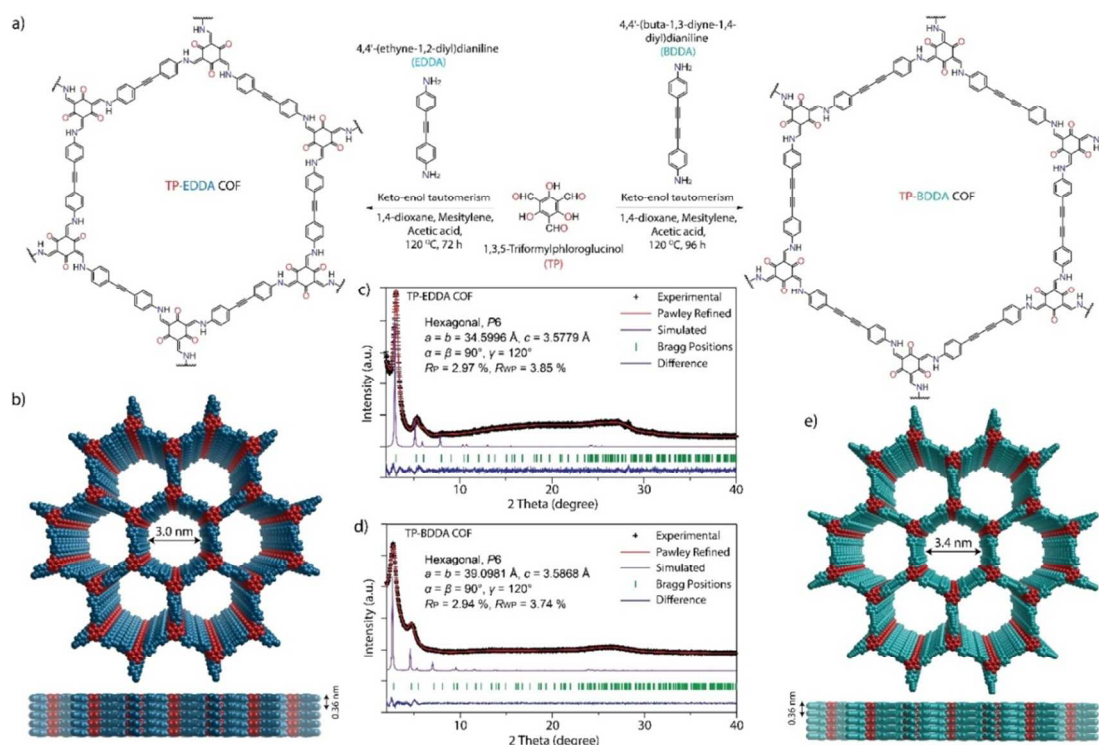


Figure 1. Synthesis and characterization of TP-EDDA and TP-BDDA COFs. (a) Scheme of the synthesis of TP-EDDA and TP-BDDA COFs. (b, e) Top and side views of TP-EDDA and TP-BDDA showing the ideal eclipsed (AA) structures. (c, d) Experimental, Pawley-refined and simulated powder X-ray diffraction patterns (AA stacking) and a difference plot for TP-EDDA and TP-BDDA COFs.

temperature. It was found that prolonging the reaction to 4 days, as compared to the typical 2 or 3 days reaction time reported for the synthesis of β -ketoenamine COFs, was necessary to yield a material with satisfactory crystallinity and long range order, confirming the above mentioned assumptions by Dichtel *et al.* on the influence of the linker size and aromaticity on the reaction rate of COF formation (Figure S3).³⁰ Notably, when the reaction was further maintained for 8 days, again a material with low crystallinity was observed, suggesting the necessity of the precise reaction time and temperature for the synthesis of crystalline TP-BDDA (Figure S3).

RESULT AND DISCUSSION

Powder X-ray diffraction (PXRD) analyses were performed to elucidate the structural features of the as-synthesized COFs. Both patterns are dominated by an intense reflection in the low-angle region, at 3.0 and 2.7 two-theta degrees for TP-EDDA and TP-BDDA, respectively, that can be assigned to the (100) facet of a primitive hexagonal lattice. Additionally, the presence of further weak reflections and a broad reflection at ~ 25 two-theta degrees for TP-EDDA and TP-BDDA COFs that can be assigned to the (001) facet, confirm the synthesis of two-dimensional COFs in a crystalline π - π stacked form (Figure 1c and 1d). The structural models for TP-EDDA and TP-BDDA were constructed by generating the expected two-dimensional hexagonal layers with **hcb** topology and modeling stacking sequences with eclipsed (AA) and staggered (AB) arrangement in the $P6$ (No. 168) and $P6_3$ (No. 173) space groups, respectively (Section S4). After geometrical optimization of the models, their simulated PXRD pattern were calculated and compared to the respective experi-

mentally measured patterns. Good agreement was found with the eclipsed stacking modes (Figure 1c and 1d, violet curves), whereas the diffraction patterns of the staggered stacking models did not reproduce the data (Figure S9, red curves), thus apparently confirming the crystallization of both the COFs in eclipsed (AA) stacking arrangement. A full profile Pawley fitting was then carried out to refine the final unit cell parameters, which has led to satisfactorily low residual values and acceptable profile differences (Figure 1c and 1d).

The permanent porosity of TP-EDDA and TP-BDDA COFs was assessed by N_2 sorption measurements at 77 K (Figure 2a). The calculated Brunauer–Emmett–Teller (BET) and Langmuir surface area values for TP-EDDA were 523 and 625 $m^2 g^{-1}$, respectively. The TP-BDDA COF showed slightly increased, but still moderate BET (758 $m^2 g^{-1}$) and Langmuir (905 $m^2 g^{-1}$) surface areas. Most probably, the low degree of π - π stacking among the adjacent COF layers, which causes an offset stacking in the framework, is responsible for the moderate surface area in TP-EDDA and TP-BDDA. A similar phenomenon has been observed previously in a diacetylene-based boronate ester COF, which was further verified using molecular dynamics and density functional theory calculations, suggesting the horizontal offset of adjacent layers by 1.7–1.8 Å.^{33,40} The completion of the reaction and the structural integrity of the framework through the formation of β -ketoenamine functionalities have been confirmed by Fourier Transform Infrared Spectroscopy (FTIR) analyses.³⁹ TP-EDDA and TP-BDDA COFs exhibit the characteristic signals corresponding to C–N and C=C bonds at ~ 1251 and ~ 1451 cm^{-1} , respectively (Figure S3). These results have been further corroborated by the ^{13}C solid-state cross-polarization magic-

angle-spinning (CP-MAS) nuclear magnetic resonance (NMR) analyses, which show the characteristic signal of the carbonyl carbon (C=O) at ~ 180 – 184 ppm and C–N bond at ~ 144 ppm, respectively (Figure 2b). The appearance of the representative signals for acetylene ($-\text{C}\equiv\text{C}-$) and diacetylene ($-\text{C}\equiv\text{C}-\text{C}\equiv\text{C}-$) functionalities for TP-EDDA and TP-BDDA COFs at ~ 87 ppm (TP-EDDA)

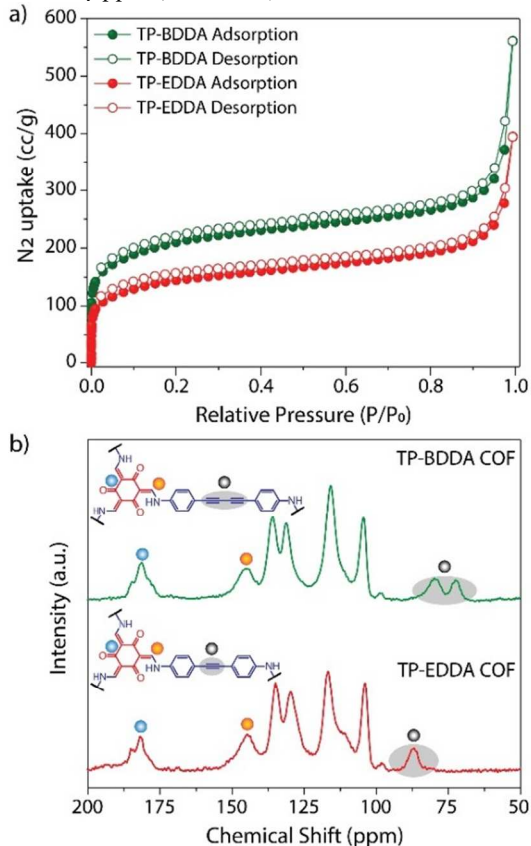


Figure 2. Characterization of TP-EDDA and TP-BDDA COFs. (a) N₂ sorption isotherms for TP-BDDA and TP-EDDA. (b) ¹³C CP-MAS solid-state NMR spectroscopy analyses of TP-BDDA and TP-EDDA.

and two signals at ~ 71 and ~ 79 ppm (TP-BDDA) validates their presence in backbones, respectively.

Scanning and transmission electron microscopy (SEM/TEM) analyses show that TP-EDDA and TP-BDDA crystallize in a flower like morphology (Figure 3a, Figure S4), where each individual crystallites have the dimensions in the hundred nanometer range. The structural stability of the solvent exchanged and as-synthesized TP-EDDA and TP-BDDA was evaluated by thermogravimetric analyses, showing a major weight loss starting at 450 °C together with some weight loss below 200 °C, probably due to the removal of trapped solvent molecules (Figure S5).

To investigate the chemical stabilities of TP-EDDA and TP-BDDA, 50 mg of each COF was submerged in various solvents. The samples were kept immersed in the respective liquids for 3 days and after washing with water analyzed for their structural stabilities. Notably, TP-BDDA and TP-EDDA retained their crystalline structure after dispersion in water, Methanol, THF, MeOH, Cyclohexanone, DMSO and DMF for 3 days (Figure 3b; Figure S6). Furthermore, the sample could be completely recovered after this treatment, thus showing no sign of decomposition and dissolution. The high stability

of the COFs in water is of course an important prerequisite for their application in photocatalytic hydrogen generation from water. Moreover, even in HCl (3 M) for 1 day, crystallinity of the COFs was essentially retained (Figure S6).

Photocatalytic hydrogen generation from water using organic semiconductors is a rapidly growing field, initiated by the discovery of visible light hydrogen evolution using

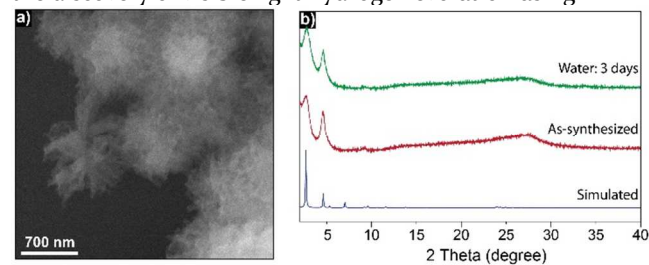


Figure 3. Characterizations of TP-BDDA. (a) SEM image of TP-BDDA showing flower-like morphologies. (b) PXRD patterns of TP-BDDA after 3 days treatment in water showing COF stability.

polymeric carbon nitride.⁴¹ Since then, several porous organic materials such as heptazine/triazine based polymers^{42–44} and conjugated microporous polymers^{45–47} are reported to exhibit hydrogen evolution activity under visible light.^{48,49} Notably, for COFs, just triazine containing frameworks have so far been shown to exhibit considerable photocatalytic activity for hydrogen evolution.^{15,50,51} Considering the significant porosity, high stability in water and presence of acetylene ($-\text{C}\equiv\text{C}-$) and diacetylene ($-\text{C}\equiv\text{C}-\text{C}\equiv\text{C}-$) functionalities in the COF backbone, the photocatalytic H₂ evolution performance of TP-EDDA and TP-BDDA was evaluated. To distinctly analyze the effect of acetylene and diacetylene moieties on optical and catalytic properties, an isorecticular COF with similar pore apertures constituted from terphenylene edges (TP-DTP COF, DTP: 4,4''-diamino-p-terphenyl) was synthesized (Section S5).^{24,52} Diffuse reflectance ultraviolet-visible spectroscopy (UV-Vis) spectra show distinct change between the COFs (Figure 4a). TP-DTP exhibits an absorbance edge around 500 nm, whereas the absorbance edge is red shifted to 520 nm and 525 nm, for TP-EDDA for TP-BDDA COFs, respectively. The absorbance tail also extended up to 675 nm for TP-BDDA, showing the distinct red shift in absorbance. Optical band gaps calculated from Tauc plots are 2.42 , 2.34 and 2.31 eV, respectively, for TP-DTP, TP-EDDA and TP-BDDA (Figure 4a, inset), which are ideal for photocatalytic water splitting, that requires a minimum band gap of ~ 1.8 eV.⁴¹

Continuous photocatalytic hydrogen evolution experiments were conducted in a Teflon reactor fitted with quartz glass window (Figure 4d, Figure S1). An optimized ratio of 9:1 for water:triethanolamine (TEOA) was used, where TEOA acts as the sacrificial electron donor to capture the photo-generated holes of the photocatalyst (Figure S21). Photo-deposited Pt (from H₂PtCl₆) acted as the co-catalyst for proton reduction. All COFs were tested for long term (10 h) hydrogen evolution under visible light (≥ 395 nm). Pressure increment due to hydrogen evolution vs time profile was recorded and subsequently converted to volume vs time profiles. TP-BDDA showed continuous hydrogen evolution over 10 h with an average rate of 324 ± 10 $\mu\text{mol h}^{-1} \text{g}^{-1}$, whereas no pressure increase was observed for both TP-EDDA and TP-DTP COF (Figure 4b). For the latter two COFs, GC results from the head space gas injection implied the production of

negligible amount of hydrogen for TP-DTP ($20 \pm 5 \mu\text{mol h}^{-1}\text{g}^{-1}$) and low hydrogen evolution for TP-EDDA ($30 \pm 5 \mu\text{mol h}^{-1}\text{g}^{-1}$) (Figure 4b and 4c). These results imply that the conjugated diacetylene moiety ($-\text{C}\equiv\text{C}-\text{C}\equiv\text{C}-$) is playing an important role for enhancing the activity for photochemical water re-

duction, which was further confirmed by photocurrent response measurement and electrochemical impedance spectroscopy analyses (Figure S22, S23). Beside lowering of the band-gap, it can be assumed

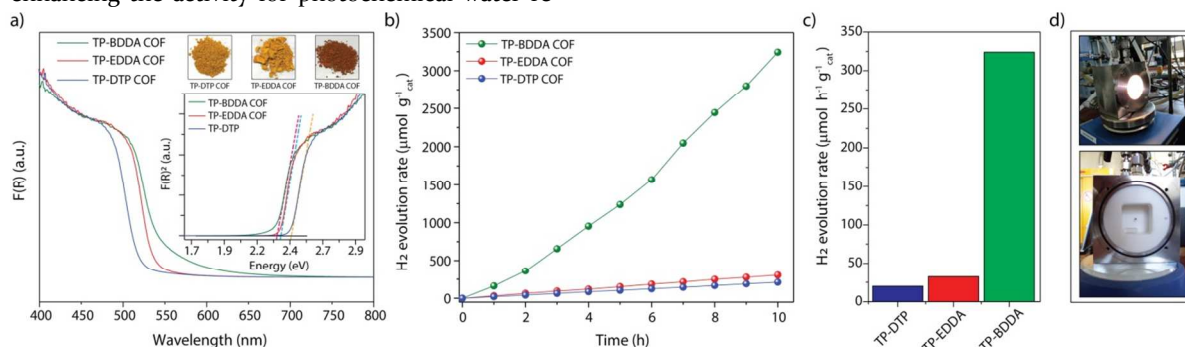


Figure 4. (a) UV-Vis diffuse reflectance spectra of TP-BDDA, TP-EDDA and TP-DTP. The inset shows Tauc plots and optical images of the COF powders. (b) Photocatalytic hydrogen evolution performance of TP-BDDA, TP-EDDA and TP-DTP catalysts under visible light irradiation ($\geq 395 \text{ nm}$) using TEOA as sacrificial agent. (c) Comparison of photocatalytic hydrogen evolution rates. (d) Reactor setup for hydrogen evolution experiments.

from studies on molecular counterparts that the diacetylene-moieties are responsible for high charge carrier mobility, i.e. for the facile migration of photogenerated excitons to the surface of the photocatalyst.^{34,36}

To quantify the photocatalytic activity of the TP-BDDA over the spectral distribution, apparent quantum efficiency (AQE) for hydrogen evolution was measured as a function of incident light wavelength using bandpass filters with central wavelength of 420 and 520 nm. A maximum apparent quantum efficiency of 1.8 was obtained with 520 nm light, which is very close to the absorbance maxima of the TP-BDDA (Figure S14 and S15). Further, a long term hydrogen evolution experiment for 60 h was conducted to elucidate the stability of the TP-BDDA catalyst (3 cycles). When TEOA was used as sacrificial agent, hydrogen evolution slightly decreases after 20 hours, however addition of fresh TEOA reactivates the system (Figure S16). After the photocatalytic experiments, recovered TP-BDDA was washed thoroughly and fully characterized by FTIR and ^{13}C CP-MAS solid state NMR spectroscopy analyses, showing complete preservation of the COF structural integrities and intact conjugated moieties within the COF backbone (Figure S17). The PXRD analyses of recovered TP-BDDA, however, showed a significant loss of long-range ordering, probably due to exfoliation of the COF nanosheets in presence of water during the photocatalysis experiments, which was reported previously also for other COFs in photocatalytic applications.^{50,53} Nonetheless, we could regenerate the crystalline material by subjecting the material after photocatalysis into the initial synthetic conditions, with characteristic peaks 40.6 and 47.1° corresponding to the Pt(o) nanoparticles (Figure S17 and S18). After photocatalysis experiments, highly dispersed Pt nanoparticles were found to be decorated (Figure S19 and S20) in TP-BDDA matrix, as confirmed the SEM and TEM analyses of the recovered sample.^{15,51,54} To confirm that the source of liberated hydrogen is indeed water, a labeling experiment was carried out with D_2O , producing D_2 in the photocatalytic experiment, as confirmed by the MS analyses of the evolved gas during photocatalysis (Figure S25).

CONCLUSIONS

In conclusion, we report the first successful preparation of porous 2D COFs including $-\text{ethyne}$ (acetylene, $-\text{C}\equiv\text{C}-$) or $-\text{buta-1,3-diyne}$ (diacetylene, $-\text{C}\equiv\text{C}-\text{C}\equiv\text{C}-$) moieties. The comparison of the photocatalytic hydrogen generation performance of TP-BDDA with acetylene (TP-EDDA) and phenyl (TP-DTP) moiety containing COFs showed the significant influence of diacetylene moieties on photocatalytic hydrogen evolution activity. To the best of our knowledge, this is a first successful demonstration of photocatalytic hydrogen generation using a COF catalyst without presence of any heteronuclear molecular functionalities (triazine- or heptazine-based moieties) inside the structure, further emphasizing the importance of the diacetylene diad in photocatalysis.

ASSOCIATED CONTENT

Supporting Information

The Supporting Information is available free of charge on the ACS Publications website at DOI: 10.1021/jacs.xxxxxx. Materials and methods, synthesis and characterization of COFs, simulation for theoretical COF structures and photocatalysis experiment details (PDF).

AUTHOR INFORMATION

Corresponding Author

*arne.thomas@tu-berlin.de

ORCID

Pradip Pachfule: 0000-0002-0804-541X

Arne Thomas: 0000-0002-2130-4930

Author Contributions

[§] P.P. and A.A. contributed equally to this work.

Notes

The authors declare no competing financial interest.

ACKNOWLEDGMENT

Support from the German Science Foundation for project TH1463/15-1 and within the Cluster of Excellence UniCat is acknowledged. P.P. thanks the Alexander von Humboldt foundation for postdoctorate fellowship. We thank Prof. M.

Antonietti, Dr. Marc Willinger, and Dr. Tobias Heil for their help in TEM analyses, and Mrs. Christina Eichenauer and Mrs. Maria Unterweger for their assistance.

REFERENCES

- (1) Barton, T. J.; Bull, L. M.; Klemperer, W. G.; Loy, D. A.; McEnaney, B.; Misono, M.; Monson, P. A.; Pez, G.; Scherer, G. W.; Vartuli, J. C.; Yaghi, O. M. *Chem. Mater.* **1999**, *11*, 2633.
- (2) Yang, X.-Y.; Chen, L.-H.; Li, Y.; Rooke, J. C.; Sanchez, C.; Su, B.-L. *Chem. Soc. Rev.* **2017**, *46*, 481.
- (3) Perego, C.; Millini, R. *Chem. Soc. Rev.* **2013**, *42*, 3956.
- (4) Chaoui, N.; Trunk, M.; Dawson, R.; Schmidt, J.; Thomas, A. *Chem. Soc. Rev.* **2017**, *46*, 3302.
- (5) Diercks, C. S.; Yaghi, O. M. *Science* **2017**, *355*, eaal1585.
- (6) Slater, A. G.; Cooper, A. I. *Science* **2015**, *348*, 988.
- (7) Davis, M. E. *Nature* **2002**, *417*, 813.
- (8) Stein, A. *Adv. Mater.* **2003**, *15*, 763.
- (9) Medina, D. D.; Sick, T.; Bein, T.; Medina, D. D.; Sick, T.; Bein, T. *Adv. Energy Mater.* **2017**, *7*, 1700387.
- (10) Pei, W. Y.; Xu, G.; Yang, J.; Wu, H.; Chen, B.; Zhou, W.; Ma, J. F. *J. Am. Chem. Soc.* **2017**, *139*, 7648.
- (11) Montoro, C.; Rodríguez-San-Miguel, D.; Polo, E.; Escudero-Cid, R.; Ruiz-González, M. L.; Navarro, J. A. R.; Ocón, P.; Zamora, F. *J. Am. Chem. Soc.* **2017**, *139*, 10079.
- (12) Zhang, J.; Han, X.; Wu, X.; Liu, Y.; Cui, Y. *J. Am. Chem. Soc.* **2017**, *139*, 8277.
- (13) Colson, J. W.; Dichtel, W. R. *Nat. Chem.* **2013**, *5*, 453.
- (14) Xu, H.; Gao, J. *Nat. Chem.* **2015**, *7*, 1.
- (15) Vyas, V. S.; Haase, F.; Stegbauer, L.; Savasci, G.; Podjaski, F.; Ochsenfeld, C.; Lotsch, B. V. *Nat. Commun.* **2015**, *6*, 8508.
- (16) Feng, X.; Ding, X.; Jiang, D. *Chem. Soc. Rev.*, **2012**, *41*, 6010.
- (17) He, T.; Pachfule, P.; Wu, H.; Xu, Q.; Chen, P. *Nat. Rev. Mater.* **2016**, *1*, 16059.
- (18) Waller, P. J.; Gándara, F.; Yaghi, O. M. *Acc. Chem. Res.* **2015**, *48*, 3053.
- (19) Huang, N.; Wang, P.; Jiang, D. *Nat. Rev. Mater.* **2016**, *1*, 16068.
- (20) Ding, S.-Y.; Wang, W. *Chem. Soc. Rev. Chem. Soc. Rev* **2013**, *42*, 548.
- (21) Zhang, Y.-B.; Su, J.; Furukawa, H.; Yun, Y.; Gándara, F.; Duong, A.; Zou, X.; Yaghi, O. M. *J. Am. Chem. Soc.* **2013**, *135*, 16336.
- (22) Segura, J. L.; Marí, A.; Mancheñ O A, J.; Lix Zamora, F. *Chem. Soc. Rev. Chem. Soc. Rev* **2016**, *45*, 5635.
- (23) Beaudoin, D.; Maris, T.; Wuest, J. D. *Nat. Chem.* **2013**, *5*, 830.
- (24) Karak, S.; Kandambeth, S.; Biswal, B. P.; Sasmal, H. S.; Kumar, S.; Pachfule, P.; Banerjee, R. *J. Am. Chem. Soc.* **2017**, *139*, 1856.
- (25) Kissel, P.; Erni, R.; Schweizer, W. B.; Rossell, M. D.; King, B. T.; Bauer, T.; Götzinger, S.; Schlüter, a. D.; Sakamoto, J. *Nat. Chem.* **2012**, *4*, 287.
- (26) Fang, Q.; Zhuang, Z.; Gu, S.; Kaspar, R. B.; Zheng, J.; Wang, J.; Qiu, S.; Yan, Y. *Nat. Commun.* **2014**, *5*, 4503.
- (27) Nagai, A.; Chen, X.; Feng, X.; Ding, X.; Guo, Z.; Jiang, D. *Angew. Chemie Int. Ed.* **2013**, *52*, 3770.
- (28) Ding, S. Y.; Gao, J.; Wang, Q.; Zhang, Y.; Song, W. G.; Su, C. Y.; Wang, W. *J. Am. Chem. Soc.* **2011**, *133*, 19816.
- (29) Kandambeth, S.; Shinde, D. B.; Panda, M. K.; Lukose, B.; Heine, T.; Banerjee, R. *Angew. Chemie Int. Ed.* **2013**, *52*, 13052.
- (30) Smith, B. J.; Hwang, N.; Chavez, A. D.; Novotney, J. L.; Dichtel, W. R. *Chem. Commun.* **2015**, *51*, 7532.
- (31) Zhu, L.; Zhang, Y.-B. *Molecules* **2017**, *22*, 1149.
- (32) Smith, B. J.; Parent, L. R.; Overholts, A. C.; Beaucage, P. A.; Bisbey, R. P.; Chavez, A. D.; Hwang, N.; Park, C.; Evans, A. M.; Gianneschi, N. C.; Dichtel, W. R. *ACS Cent. Sci.* **2017**, *3*, 58.
- (33) Spittler, E. L.; Koo, B. T.; Novotney, J. L.; Colson, J. W.; Uribe-Romo, F. J.; Gutierrez, G. D.; Clancy, P.; Dichtel, W. R. *J. Am. Chem. Soc.* **2011**, *133*, 19416.
- (34) Ghosh, S.; Kouamé, N. A.; Ramos, L.; Remita, S.; Dazzi, A.; Deniset-Besseau, A.; Beaunier, P.; Goubard, F.; Aubert, P.-H.; Remita, H. *Nat. Mater.* **2015**, *14*, 505.
- (35) Jayanthi, S.; Muthu, D. V. S.; Jayaraman, N.; Sampath, S.; Sood, A. K. *ChemistrySelect* **2017**, *2*, 4522.
- (36) Planells, M.; Abate, A.; Hollman, D. J.; Stranks, S. D.; Bharti, V.; Gaur, J.; Mohanty, D.; Chand, S.; Snaith, H. J.; Robertson, N. *J. Mater. Chem. A* **2013**, *1*, 6949.
- (37) Beckham, H. W.; Rubner, M. F. *Polymer* **1991**, *32*, 1821.
- (38) Maeda, K.; Hong, L.; Nishihara, T.; Nakanishi, Y.; Miyachi, Y.; Kitaura, R.; Ousaka, N.; Yashima, E.; Ito, H.; Itami, K. *J. Am. Chem. Soc.* **2016**, *138*, 11001.
- (39) Kandambeth, S.; Mallick, A.; Lukose, B.; Heine, T.; Banerjee, R.; Mane, M. *J. Am. Chem. Soc.* **2012**, *134*, 19524.
- (40) Lukose, B.; Kuc, A.; Heine, T. *Chem. - A Eur. J.* **2011**, *17*, 2388.
- (41) Wang, X.; Maeda, K.; Thomas, A.; Takanabe, K.; Xin, G.; Carlsson, J. M.; Domen, K.; Antonietti, M. *Nat. Mater.* **2009**, *8*, 76.
- (42) Kailasam, K.; Schmidt, J.; Bildirir, H.; Zhang, G.; Blechert, S.; Wang, X.; Thomas, A. *Macromol. Rapid Commun.* **2013**, *34*, 1008.
- (43) Schwarz, D.; Kochergin, Y. S.; Acharja, A.; Ichangi, A.; Opanasenko, M. V.; Čejka, J.; Lappan, U.; Arki, P.; He, J.; Schmidt, J.; Nachtigall, P.; Thomas, A.; Bojdys, M. *J. Chem. - A Eur. J.* **2017**, *23*, 13023.
- (44) Kailasam, K.; Mesch, M. B.; Möhlmann, L.; Baar, M.; Blechert, S.; Schwarze, M.; Schröder, M.; Schomäcker, R.; Senker, J.; Thomas, A. *Energy Technol.* **2016**, *4*, 744.
- (45) Sprick, R. S.; Jiang, J. X.; Bonillo, B.; Ren, S.; Ratvijitvech, T.; Guiglion, P.; Zwijnenburg, M. A.; Adams, D. J.; Cooper, A. I. *J. Am. Chem. Soc.* **2015**, *137*, 3265.
- (46) Sprick, R. S.; Bonillo, B.; Clowes, R.; Guiglion, P.; Brownbill, N. J.; Slater, B. J.; Blanc, F.; Zwijnenburg, M. A.; Adams, D. J.; Cooper, A. I. *Angew. Chemie Int. Ed.* **2016**, *55*, 1792.
- (47) Li, L.; Cai, Z.; Wu, Q.; Lo, W. Y.; Zhang, N.; Chen, L. X.; Yu, L. *J. Am. Chem. Soc.* **2016**, *138*, 7681.
- (48) Zhang, P.; Song, T.; Wang, T.; Zeng, H. *Int. J. Hydrogen Energy* **2017**, *42*, 14511.
- (49) Song, T.; Zhang, L.; Zhang, P.; Zeng, J.; Wang, T.; Ali, A.; Zeng, H. *J. Mater. Chem. A* **2017**, *5*, 6013.
- (50) Stegbauer, L.; Schwinghammer, K.; Lotsch, B. V. *Chem. Sci.* **2014**, *5*, 2789.
- (51) Kuecken, S.; Acharjya, A.; Zhi, L.; Schwarze, M.; Schomäcker, R.; Thomas, A. *Chem. Commun.* **2017**, *53*, 5854.
- (52) Zhu, Y.; Zhang, W. *Chem. Sci.* **2014**, *5*, 4957.
- (53) Bunck, D. N.; Dichtel, W. R. *J. Am. Chem. Soc.* **2013**, *135*, 14952.
- (54) Zhang, G.; Lan, Z.-A.; Lin, L.; Lin, S.; Wang, X. *Chem. Sci.* **2016**, *7*, 3062.

TOC IMAGE

